The cost effectiveness of electrodialysis for diverse salinity applications

Citation: McGovern, Ronan K., Syed M. Zubair, and John H. Lienhard V. "The Cost Effectiveness of Electrodialysis for Diverse Salinity Applications." Desalination 348 (September 2014): 57–65.

As Published: http://dx.doi.org/10.1016/j.desal.2014.06.010

Publisher: Elsevier

Persistent URL: http://hdl.handle.net/1721.1/102495

Version: Author's final manuscript: final author's manuscript post peer review, without publisher's formatting or copy editing

The cost effectiveness of electrodialysis for diverse salinity applications

Ronan K. McGovern[a], Syed M. Zubair[b], John H. Lienhard V[a]

[a]*Center for Clean Water and Clean Energy, Massachusetts Institute of Technology, Cambridge, MA 02139, United States*
[b]*King Fahd University for Petroleum and Minerals, Dhahran, Saudi Arabia*

Abstract

We provide a thermoeconomic assessment of electrodialysis indicating that the technology is most productive and efficient for the partial desalination of feed streams at the higher end of the brackish range of salinities. After optimising the current density to minimise the sum of energy and equipment costs, we demonstrate that at low feed salinities the productivity, and hence equipment costs, of electrodialysis are hampered by the limiting current density. By contrast, at higher feed salinities both productivity and efficiency are hampered by the reduced chemical potential difference of salt in the diluate (low salinity) and concentrate (high salinity) streams. This analysis indicates the promise of further developing electrodialysis for the treatment of waters from oil, gas and coal-bed methane as well as flue-gas de-sulphurisation, where the partial desalination of streams at the high-end of the brackish range can be beneficial.

Keywords: electrodialysis, productivity, efficiency, cost

1. Introduction

Electrodialysis involves the transfer of ions from a low salinity stream to a higher salinity stream — from diluate to concentrate. Together, the diluate salinity, the difference between diluate and concentrate salinity, and the ratio of concentrate-to-diluate salinity capture, via their effects on salt and water transport, the influence of salinity on cost. Our objective is to demonstrate that these three factors determine the influence of salinity on the cost-effectiveness of electrodialysis, and furthermore, that they have driven and will drive the selection of applications for which ED is worthy of development.

Recently, significant attention has been paid to the development of new electrical desalination methods [1–4], some of which report experimentally measured energy consumption close to reversible [2, 4–6] and some of which report extraordinarily high salt removal rates per unit area [2, 6]. Given the early stage of development of these technologies, there are interesting questions around their cost competitiveness at larger scales and, of interest in the present context, the range of salinities for which they are most economical. By analysing the effect of salinity upon the cost effectiveness of electrodialysis, a precedent is established allowing similar analyses to be conducted for emerging technologies as system models are developed.

No existing unified framework is available to explain, in a general sense, how diluate and concentrate salinities affect the cost of electrodialysis — though literature does provide certain distinct insights into the effects of salinity. At low diluate salinity, salt removal is restricted by the limiting current density and ohmic resistance is high. For brackish water desalination [7, 8], and to a lesser extent salt production [9], the limiting current density effectively sets the size of equipment required. For the purification of higher salinity streams such as seawater [10] or produced water [11], currents are lowest (and, we surmise, capital costs highest) in the final stages of purification. High diluate resistance results in elevated energy consumption for brackish desalination, particularly due to the dominance of solution resistances over membrane resistances. Indeed, the challenges posed by a low diluate salinity are largely responsible for the development of narrow membrane channels [12], ion-conductive spacers within diluate channels (electrodeionisation) [13, 14], hybrid designs combining ED with reverse osmosis [15–17], and theories to understand and possibly extend the operation of ED into the overlimiting current region [18]. With a large salinity difference between diluate and concentrate salinity, back diffusion of salt and water transport by osmosis degrade performance. In brackish desalination applications, this effect, coupled with the risk of scale formation at high concentrations, limits the recovery of feed water as a purified product. In concentrative applications, osmosis and diffusion serve to reduce the maximum concentration achievable in combination with the effect of water transport by electroosmosis [19–22].

Email addresses: mcgov@alum.mit.edu (Ronan K. McGovern), lienhard@mit.edu (John H. Lienhard V)

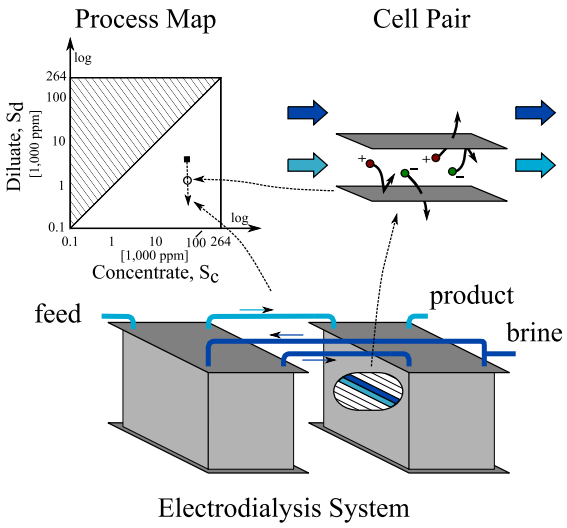

Figure 1: Anti-clockwise from bottom: an ED system; an ED cell pair; and a salinity map illustrating a desalination process. The process within an infinitesimal cell pair is represented by a point on the salinity map. The ED system, comprised of multiple cell pairs, is represented by a line on the salinity map.

Our objective is to draw together the above insights and propose a unified framework explaining the influence of salinity upon the cost of electrodialysis [1]. Rather than modelling, in detail, a variety of electrodialysis processes, our approach is to consider a short cell pair that can represent a portion of any electrodialysis process.

2. Methodology

By understanding how the performance and cost of a short cell pair depend upon diluate and concentrate salinity, we can understand how overall systems will perform across different salinity ranges. Figure 1 illustrates how the process in a two stage brackish water desalination system may be represented on a salinity map, and furthermore, how a short cell pair at any point in the system is represented by a point along the process path. Our approach consists of mapping the cost of this short cell pair process over the entire range of diluate and concentrate salinities. The consequent map of cost then allows us to assess the cost effectiveness of diverse ED processes.

To construct a map of cost we consider a numerical model of a short cell pair that allows us to parametrise diluate and concentrate salinity. We first establish a metric for the cost of separation. We then present a model for local salt transport, water transport and cell pair voltage. Finally, coupling these cost and cell pair models, and optimising for current density, we parametrise diluate and concentrate salinity to numerically investigate how they influence the 'Local Cost'.

2.1. The 'Local Cost' of separation

In a detailed analysis, costs associated with membrane replacement, chemical usage, the replacement of miscellaneous parts and pre-treatment might be considered [23]. In this analysis we focus upon equipment and energy costs and determine the cost per unit time of operating an incremental cell pair as follows:

$$\text{Cost per unit time} = \frac{K_Q \delta A^{cp}}{CAF} + K_E \delta P \qquad (1)$$

Equipment costs are formulated as the product of a specific equipment cost per unit cell pair area K_Q and the incremental cell pair area δA^{cp} (with δ signifying an increment), together divided by the capital amortisation factor CAF — which allows for a return on the investment in equipment:

$$CAF = \frac{1}{r}\left[1 - \left(\frac{1}{1+r}\right)^{\tau}\right] \qquad (2)$$

Energy costs in Eq. (1) are formulated as the product of electricity price, K_E, and the incremental power consumption of the cell pair δP. Pumping power costs, typically smaller than stack power consumption in brackish [7] and salt production applications [9], are not considered as we focus on the trade-off between stack power and system size. Relative to stack power consumption, pumping power is most significant at low diluate salinity where the current density and hence the stack power density is small. That pumping power is a low fraction of total power at low salinity thus suggests that this should also be the case at higher salinities [7, 24].

Setting pumping power aside, power consumption in the cell pair is therefore given by the product of cell pair voltage, V^{cp}, current density, i, and incremental cell pair area:

$$\delta P = i V^{cp} \delta A^{cp} \qquad (3)$$

Given the incremental cost of operating a cell pair we next establish a basis upon which this cost can be made specific. We consider costs on the basis of the rate of change in free energy of process streams. For a short (infinitesimal) cell pair, this rate of change is given by:

$$\delta G = \delta \dot{N}_s \Delta\mu_s + \delta \dot{N}_w \Delta\mu_w \qquad (4)$$

where $\delta \dot{N}_s$ and $\delta \dot{N}_w$ are incremental molar flow rates of salt and water through the membranes, respectively, and μ denotes chemical potential, which takes the form

[1] A similar approach might also be applied to analyse power generation with reverse electrodialysis technology, but here we focus upon electrodialysis.

of:

$$\mu_s - \mu_s^0 = RT \ln(\gamma m) \tag{5}$$

$$\mu_w - \mu_w^0 = RT\phi M_w \nu m \tag{6}$$

for salt and water respectively, with R the universal gas constant, T the temperature, γ the mean molal salt activity coefficient, m the molal concentration of salt, ν the number of moles of dissociated ions per mole of salt (2 for NaCl), ϕ the osmotic coefficient, μ_s^0 the chemical potential of salt in its reference state and μ_w^0 the chemical potential of water in its reference state.

The cost basis of free energy change, rather than water removal (*e.g.*, \$/m^3 of water) or salt removal (*e.g.*, \$/kg of salt), is based on the thermodynamic consideration that the difficulty of salt (or water) removal depends upon salinity. The difficulty of salt removal, as measured by the change in chemical potential in Fig. 2a, is greater when salt is removed (say into a saturated solution) from a lower salinity stream. By contrast, the removal of water (in pure form) is more difficult from a higher salinity stream. Given the incremental cost of operating a cell pair and the incremental rate of change of free energy we define the 'Specific Local Cost' of separation as follows:

$$SLCS = \frac{\frac{K_Q \delta A^{cp}}{CAF} + K_E \delta P}{\dot{N}_s \Delta\mu_s + \dot{N}_w \Delta\mu_w}. \tag{7}$$

Dividing across by K_E and defining the equipment-to-energy price ratio as:

$$R_p = \frac{K_Q}{CAF}\frac{1}{K_E} \tag{8}$$

we obtain a simple expression for the dimensionless 'Local Cost' of separation:

$$Local\ Cost = \frac{SLCS}{K_E} = \frac{R_p \delta A^{cp}}{\dot{N}_s \Delta\mu_s + \dot{N}_w \Delta\mu_w} + \frac{\delta P}{\dot{N}_s \Delta\mu_s + \dot{N}_w \Delta\mu_w} \tag{9}$$

This expression, which for brevity we will term 'Local Cost', represents the comparison of the price of a unit change in free energy to the price of a unit of electricity. Further examination of Eq. (9) allows us to write the 'Local Cost' as:

$$Local\ Cost = \frac{SLCS}{K_E} = \frac{R_p}{\xi} + \frac{1}{\eta} \tag{10}$$

with productivity ξ defined as the incremental rate of change of free energy per unit system area (*e.g.*, cell pair area for ED):

$$\xi = \frac{\dot{N}_s \Delta\mu_s + \dot{N}_w \Delta\mu_w}{\delta A^{cp}} = J_s \Delta\mu_s + J_w \Delta\mu_w \tag{11}$$

and efficiency defined as the ratio of the productivity to the area normalised power input:

$$\eta = \frac{J_s \delta A^{cp} \Delta\mu_s + J_w \delta A^{cp} \Delta\mu_w}{i V^{cp} \delta A^{cp}} = \frac{\xi}{i V^{cp}}. \tag{12}$$

J denotes a transmembrane molar flux, i denotes current density and V^{cp} denotes cell pair voltage. Of particular importance, both for productivity and efficiency, are the changes in chemical potential of water and salt during transport. We can see, according to Fig. 2a, that the productivity of salt removal systems is poor when removing salt from low salinity solutions while, according to Fig. 2b, the productivity of water removal systems is poor when removing water from low salinity solutions. Thus, we establish that small changes in chemical potential of species during transport results in poor productivity and, if the denominator of Eq (12) were constant, poor efficiency. Furthermore we can see that water transport from diluate to concentrate and salt transport from concentrate to diluate in electrodialysis reduces productivity.

2.2. The cell pair model

The key outputs of the cell pair model, required to determine 'Local Cost', are the salt flux, J_s, water flux, J_w, and the cell pair voltage, V^{cp}. Together these three quantities allow the determination of productivity and efficiency (Eqs. (11) and (12)), which in turn determine 'Local Cost' in Eq. (10).

Salt and water transport are modelled based upon the approach taken by Fidaleo and Moresi [20]. Salt transport is modelled by a combination of migration and diffusion:

$$J_s = \frac{T_s^{cp} i}{F} - L_s \left(C_{s,c,m} - C_{s,d,m}\right) \tag{13}$$

and water transport by a combination of migration (electro-osmosis) and osmosis:

$$J_w = \frac{T_w^{cp} i}{F} + L_w \left(\pi_{s,c,m} - \pi_{s,d,m}\right) \tag{14}$$

T_s^{cp} and T_w^{cp} are the overall salt and water transport numbers for the cell pair. L_s and L_w are the overall salt and water permeabilities of the cell pair. C denotes concentration in moles per unit volume and π osmotic pressure. The difference between bulk and membrane wall concentrations and osmotic pressures is accounted for by a convection-diffusion model of concentration polarisation [26]:

$$\Delta C = -\frac{\left(\bar{T}_{cu} - t_{cu}\right)}{D}\frac{i}{F}\frac{2h}{\mathrm{Sh}} \tag{15}$$

where t_{cu} is the counter-ion transport number in solutions and is approximated as 0.5 for both anions and

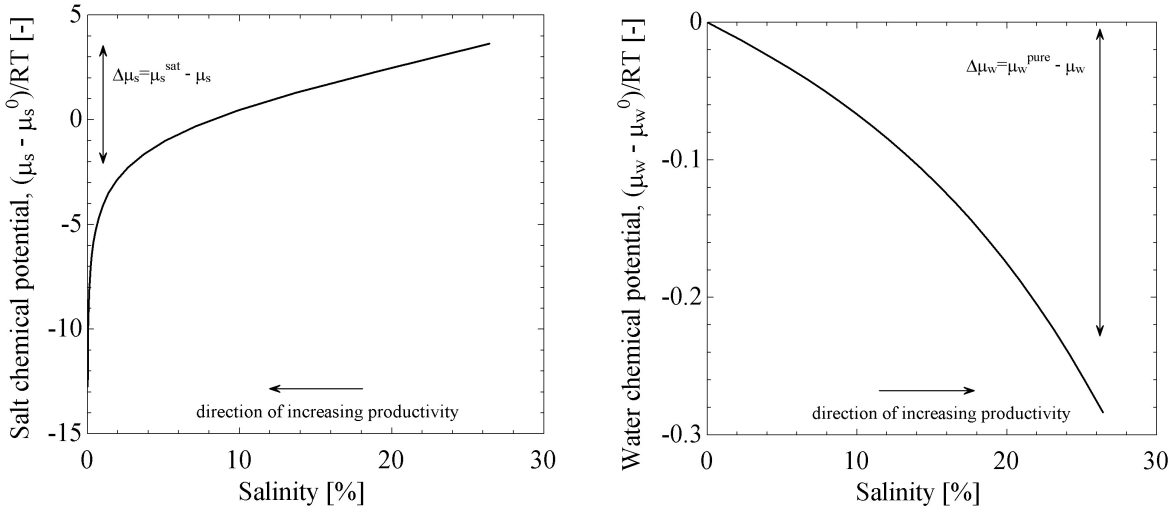

(a) Sodium chloride chemical potential

(b) Water chemical potential

Figure 2: Chemical potentials of sodium chloride and water in an aqueous NaCl and water solution as a function of salinity. Osmotic coefficient and NaCl activity coefficient data from Robinson and Stokes [25]

cations. $\bar{T}_{cu}$ is the integral counter-ion transport number in the membrane that accounts for both migration and diffusion and is modelled as follows:

$$\bar{T}_{cu} \approx \frac{T_s^{cp} + 1}{2}. \tag{16}$$

This expression is exact if diffusion within the membrane is negligible and the counter-ion transport number is equal in the anion and cation exchange membranes. The cell pair voltage, Fig. 3, is represented as the sum of ohmic terms, membrane potentials and junction potentials:

$$V^{cp} = i\,(\bar{r}_{am} + \bar{r}_{cm} + \bar{r}_d + \bar{r}_c) + E_{am} + E_{cm} + \sum E_j \tag{17}$$

Membrane surface resistances are considered to be independent of salinity. The surface resistances of the diluate and concentrate solutions are computed considering the channel height and the bulk solution conductivity:

$$\bar{r}_d + \bar{r}_d = \frac{h_d}{k_d} + \frac{h_c}{k_c} = \frac{h_d}{\Lambda_d C_d} + \frac{h_c}{\Lambda_c C_c} \tag{18}$$

where Λ is the molar conductivity, itself a function of concentration [27, 28]. Concentration polarisation boundary layers are symmetric, since $\bar{T}_{cu}$ and t_{cu} are approximated as equal for anion and cation exchange membranes, and anions and cations, respectively. Thus, the junction potentials cancel within each channel. Finally, the sum of the anion and cation membrane potentials is computed considering quasi-equilibrium migration of salt and water across the membranes:

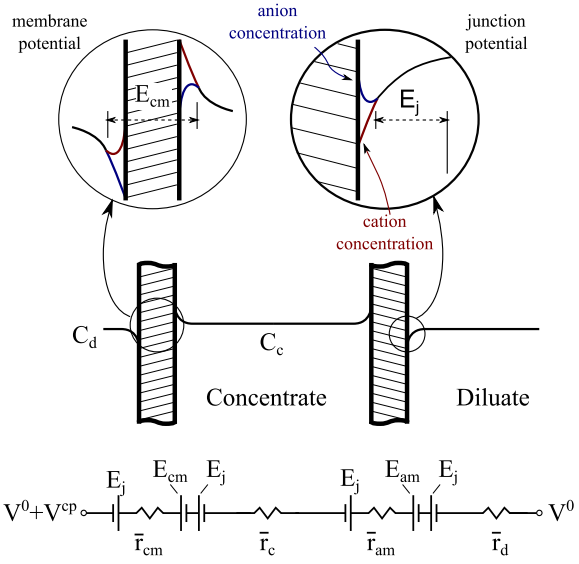

Figure 3: Representation of the voltage drop and concentration change across a single cell pair

$$E_{am}+E_{cm} = \frac{T_s^{cp}}{F}(\mu_{s,c,m} - \mu_{s,d,m}) + \frac{T_w^{cp}}{F}(\mu_{w,c,m} - \mu_{w,d,m}) \tag{19}$$

2.3. The input parameters to the numerical model

To investigate the dependence of 'Local Cost' upon diluate and concentrate salinity, we select representative values from literature as inputs to the cell pair and

Symbol	Value	Ref.
Membrane Performance Parameters		
T_s	0.97	[29][2]
T_w	10	[29]
L_w	1.4×10^{-4} mol/bar-m^2-s	[29]
L_s	1.4×10^{-8} m/s	[29]
$\bar{r}_{am}$	2.8 Ω cm^2	[29]
$\bar{r}_{cm}$	2.8 Ω cm^2	[29]
Solution Properties		
D	1.61×10^{-9} m^2/s	[25]
t_{cu}	0.5	[30]
Flow Properties		
h	0.7 mm	[7, 29]
Sh	20	[7, 29]

Table 1: Membrane performance, solution and flow properties. For channel height, Lee et al. [7] suggest 0.65 mm, while Fidaleo et al. [29] employ 0.7 mm. For Reynolds number Lee et al. [7] suggest Re_{D_h} of approximately 100, while Fidaleo et al. [29] employ a Reynolds of approximately 25 to 50. Taken together with Fidaleo et al.'s Sherwood number correlation, $\mathrm{Sh} = 0.37 \cdot Re_{D_h}^{1/2} Sc^{1/3}$, with Sc ≈ 620, yields Sh in the range of 12-22.

Symbol	Value	Ref.
K_{EQ}	300 \$/m^2 cell pair	[7, 8]
τ	20 years	-
r	5%	[31]
LCE	0.065 \$/kWh	[32]

Table 2: Cost model parameters

cost models (Tables 1 and 2) respectively.

The salinity dependence of membrane performance parameters is membrane specific and data is not widely available for cell pairs[3]. No salinity dependence of membrane performance parameters is included, as a result of which, in particular due to the assumed high permselectivity of anion and cation membranes, this analysis provides a lower bound on cost at higher salinities. Flow conditions are taken as constant, meaning viscous dissipation per unit cell pair area (relating to pumping power requirements) is unaffected[4] by diluate or concentrate salinity. The area normalised equipment cost is chosen in line with Lee et al. [7], and doubled to convert from m^2 membrane area to m^2 cell pair area. A cost of capital of 5% is considered, guided by the 4.78% interest rate paid to construction bondholders for the Carlsbad desalination plant [31]. Finally, the levelised cost of electricity cost is representative of the levelized cost of combined cycle natural gas-fired power plants, including transmission investments, coming online in 2018 [32].

[3]Data is available for cation exchange membranes [33, 34]

[4]Strictly, salinity affects viscosity, resulting in a second order effect upon viscous dissipation

3. Dependence of efficiency, productivity and cost upon current density for fixed salinities

There are two layers to the analysis of the 'Local Cost': the first is the optimisation of current density for fixed bulk salinities; the second, to be seen in Section 4, is the analysis of how diluate and concentrate salinity affect 'Local Cost'.

To illustrate the dependence of productivity and efficiency on current density we can combine Eqs. (13), (14) and (17) into Eqs. (11) and (12) to give:

$$\xi = C_{mig} i - C_{od} \tag{20}$$

$$\eta = \frac{C_{mig} i - C_{od}}{C_{mp} i + C_{oh} i^2} \tag{21}$$

where C_{mig}, C_{od}, C_{mp} and C_{oh} are pre-factors that relate to salt and water migration, osmosis and salt diffusion, membrane potentials and ohmic resistances respectively. C_{mig} and C_{oh} depend upon bulk salinities while C_{od} and C_{mp} depend upon salinities at membrane surfaces, and thus, via concentration polarisation, are implicit functions of current density. Considering:

$$S = \frac{M_s C}{\rho} \approx \frac{M_s m}{\rho}, \tag{22}$$

the approximate dependence of each pre-factor upon salinity is:

$$C_{mig} = \frac{1}{F}[t_s^{cp} \underbrace{(\mu_{s,c} - \mu_{s,d})}_{\sim \ln\left(\frac{S_c}{S_d}\right)} + t_w^{cp} \underbrace{(\mu_{w,c} - \mu_{w,d})}_{\sim -\ln\left(\frac{S_c}{S_d}\right)}] \tag{23}$$

$$\begin{aligned} C_{od} =& L_w \underbrace{(\pi_{c,m} - \pi_{d,m})(\mu_{w,d} - \mu_{w,c})}_{\sim (S_{c,m} - S_{d,m})(S_c - S_d)} \\ &+ L_s \underbrace{(C_{s,c,m} - C_{s,d,m})(\mu_{s,c} - \mu_{s,d})}_{\sim (S_{c,m} - S_{d,m}) \ln\left(\frac{S_c}{S_d}\right)} \end{aligned} \tag{24}$$

$$C_{oh} = \bar{r}_{am} + \bar{r}_{cm} + \underbrace{\bar{r}_d}_{\sim \frac{1}{S_d}} + \underbrace{\bar{r}_c}_{\sim \frac{1}{S_c}} \tag{25}$$

$$\begin{aligned} C_{mp} =& \frac{t_s^{cp}}{F} \underbrace{(\mu_{s,c,m} - \mu_{s,d,m})}_{\sim \ln\left(\frac{S_{c,m}}{S_{d,m}}\right)} \\ &+ \frac{t_w^{cp}}{F} \underbrace{(\mu_{w,c,m} - \mu_{w,d,m})}_{\sim -(S_{c,m} - S_{d,m})} \end{aligned} \tag{26}$$

To obtain the simplified expressions for each of the above pre-factors we have taken osmotic and salt activity coefficients as unity[5] and linearised the relationship between salinity and concentrations. In Section 4 we

[5]The osmotic coefficient of aqueous NaCl varies between a minimum of 0.92 and a maximum of 1.27, and the NaCl activity coefficient between 0.65 and 1.00, over the range from an infinitely dilute to a saturated solution [25].

will analyse the dependence of these pre-factors upon diluate and concentrate salinity. At this point, we focus on how current density affects efficiency and productivity for constant diluate and concentrate salinities (Fig. 4a and 4b).

At low current densities both productivity and efficiency improve as the free energy change associated with migration increases relative to migration and diffusion. As a consequence, regardless of the price ratio R_p in Eq. (10), it would never be sensible, from a cost perspective, to operate at a current density below about 12 A/m^2. At higher current densities, up until the limiting current density of about 55 A/m^2, productivity increases while efficiency decreases with increasing current density. These trends give rise to an important trade-off between productivity and efficiency, as seen in Eq. (10) and in Fig. 4c, whereby an increase in current density gives rise to an increase in energy costs but a decrease in equipment costs. Ultimately, the relative importance of achieving high productivity versus high efficiency is set by the price ratio, R_p, of equipment to energy costs. Interestingly, at a value of $R_p = 42.3$ W/m^2, the optimal current density (about 50 A/m^2) is very close to the limiting current density; consistent with industrial practice in brackish water desalination where the current density is set close to its limiting value [7].

4. Dependence of productivity, efficiency and cost upon salinities at the optimal current density

From here on, in analysing the effect of diluate and concentrate salinities, we consider only the value of current density that minimises the 'Local Cost' for a given diluate-concentrate salinity pair. In other words, the current density is always chosen to optimise the trade-off between productivity and efficiency. The current-optimised 'Local Cost*' for each diluate-concentrate salinity pair is thus given, combining Eqs. (10), (20) and (21), by:

$$Local\ Cost^* = \min_i \frac{R_p}{C_{mig} i - C_{od}} + \frac{C_{mp} i + C_{oh} i^2}{C_{mig} i - C_{od}}. \tag{27}$$

with an asterisk indicating that the current density has been optimised. Figure 5 illustrates the effect of both diluate and concentrate salinities upon the optimal productivity, efficiency, 'Local Cost*' and current density, solved for numerically, in each case, using a quadratic approximations method in Engineering Equation Solver [35]. There are four important trends to observe, which we will explain in the following subsections:

1. For any value of diluate salinity, there exists a value of concentrate salinity that minimises 'Local Cost*' — since both productivity and efficiency exibit maxima at lower diluate salinities and efficiency exhibits a maximum for any diluate salinity. Furthermore, that the optimal concentrate salinity decreases as the diluate salinity decreases supports the logic of operating electrodialysis stacks with the diluate and concentrate in counterflow [36].
2. There exists a diluate-concentrate pair that minimises the 'Local Cost*' — roughly because efficiency falls at higher diluate salinities and productivity rises at lower salinities.
3. For fixed diluate salinity, the optimal current density increases with increasing concentrate salinity.
4. For fixed concentrate salinity, the optimal current density increases with increasing diluate salinity at low diluate salinities but decreases at high diluate salinities.

4.1. Influence of salinities upon productivity, efficiency and 'Local Cost*'

To understand why there is an optimal concentrate salinity for each diluate salinity and why there is an overall optimal diluate-concentrate salinity pair we examine the influence of salinity upon productivity (Eq. (20)), efficiency (Eq. (21)) and 'Local Cost*' (Eq. (27)). To do this we return to Eqs. (23), (24), (25) and (26). Fig. 6 provides a graphical illustration of these equations to further help understand the relationships between the four pre-factors and the diluate and concentrate salinity. It is arrived at by considering that:

(A) C_{mig} becomes low when the salinity ratio S_c/S_d becomes low. This is qualitatively represented in Fig. 6 by a line of constant salinity ratio above which the change in free energy associated with migration is low. Since the concentrate salinity is limited by the salinity of the solution at saturation, high diluate salinities (or feed salinities to a system) are synonymous with low salinity ratios.

(B) C_{od} becomes high when there is significant separation between diluate and concentrate salinity. This is represented in Fig. 6 by a line of constant salinity difference to the right of and below which the effects of osmosis and diffusion are strong.

(C) C_{oh} becomes high at low diluate salinity. This is represented in Fig. 6 by a line of constant diluate salinity below which ohmic resistance is high.

(D) C_{mp} has a similar dependence upon salinities as C_{mig} but differs in that its value must always be greater due to concentration polarisation. This difference is primarily important at low diluate salinity where the salinity difference $\Delta S = S_d - S_{d,m}$ has a strong effect upon the denominator of the first term on the right hand side of Eq. (26). Thus, the region where C_{mp}/C_{mig} is high is represented in Fig. 6 by illustrating a horizontal line of

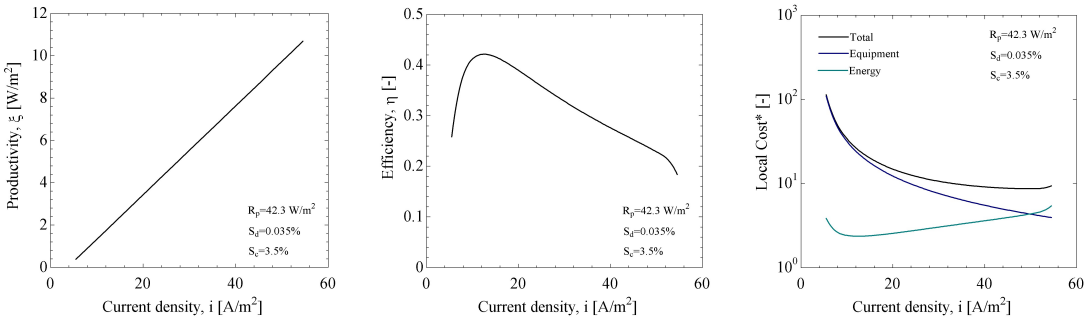

(a) Productivity (b) Efficiency (c) Cost

Figure 4: Influence of current density upon efficiency, productivity and cost

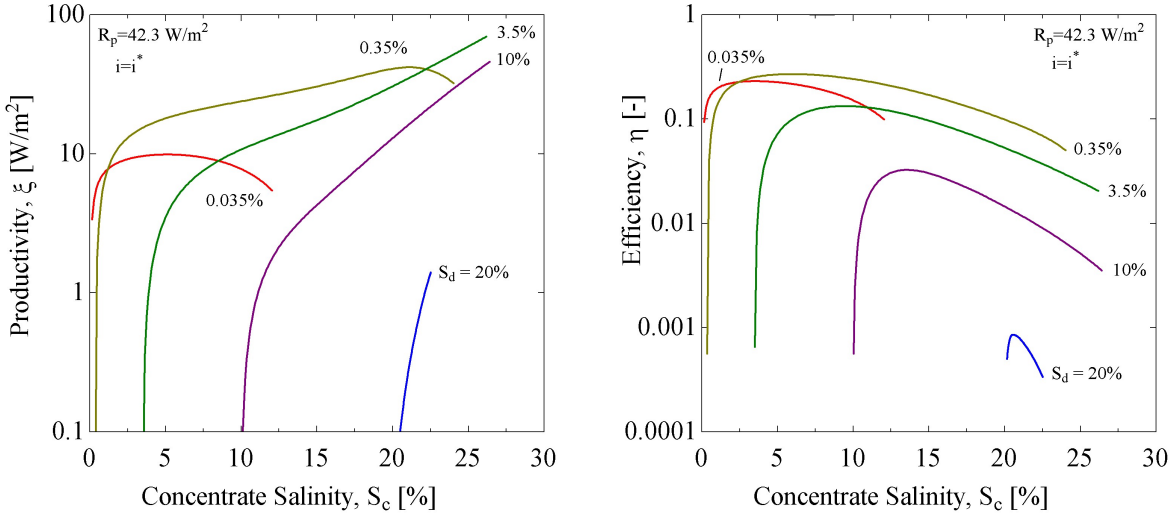

(a) Productivity (b) Efficiency

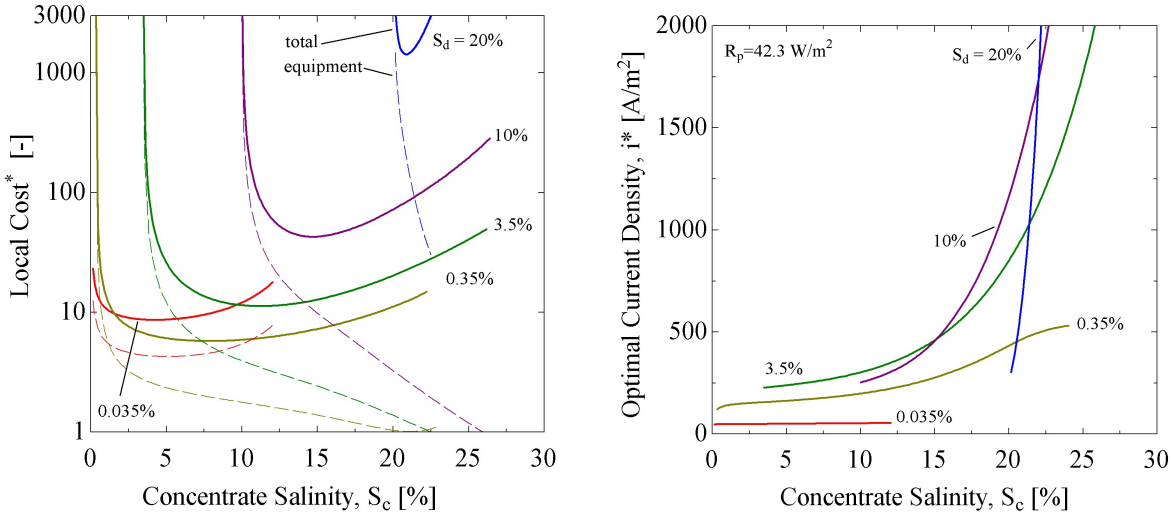

(c) Dimensionless local specific cost (d) Optimal current density

Figure 5: Influence of diluate and concentrate salinity upon efficiency, productivity, 'Local Cost*' and optimal current density

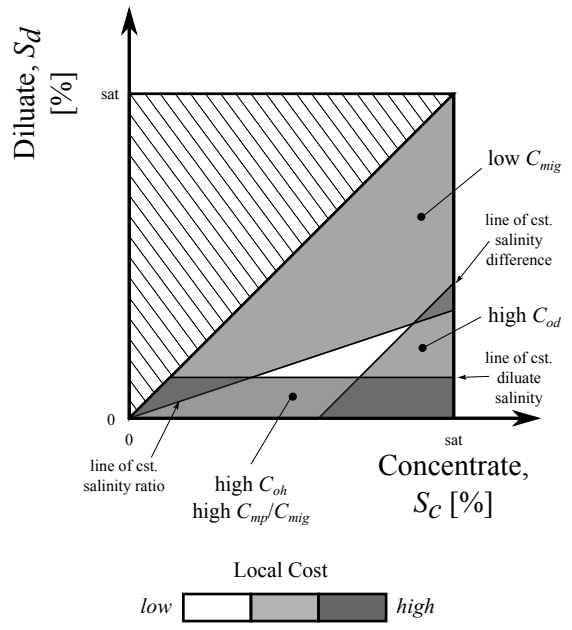

Figure 6: Dimensionless local specific cost

constant diluate salinity (the same line as for C_{oh}), below which concentration polarisation results in a deviation of C_{mp} above C_{mig}[6].

Given this understanding we can return to Eqs. (10), (20) and (21) to see how, for a fixed diluate salinity, low concentrate salinities result in low C_{mig} (low salinity ratios) and consequently reduce efficiency, productivity and 'Local Cost*', while high concentrate salinities result in high values of C_{od} (high salinity differences) and consequently also reduce efficiency, productivity and 'Local Cost*'. Hence, for fixed diluate salinity, intermediate values of concentrate salinity lead to minimum 'Local Cost*'.

Secondly, we can understand how low values of diluate salinity lead to high C_{oh} and high C_{mp}/C_{mig} while high values of diluate salinity make high salinity ratios, and hence high C_{mig} unachievable. This explains the existence of a single diluate-concentrate pair that minimises the 'Local Cost*'. In summary, there are three primary drivers of high 'Local Cost*' for electrodialysis:

1. A low salinity ratio (synonymous with high diluate or system feed salinities) — resulting in poor productivity
2. A large difference between diluate and concentrate salinity — resulting in high diffusion and osmosis
3. A low diluate salinity — resulting in significant ohmic resistance and concentration polarisation

4.2. Influence of salinities on optimal current density

To understand trends in the optimal current density with diluate and concentrate salinity we analyse the solution to Equation (27), which makes apparent the dependence of 'Local Cost*' upon current density. C_{mp} and, to a lesser extent, C_{od}, are functions of current density since they depend upon concentrations at membrane surfaces. This makes it impossible to obtain an exact analytical solution for the optimal current density. However, considering cases where concentration polarisation is negligible, and thus $C_{mp} \approx C_{mig}$, the optimal current density is given analytically by:

$$i^* = \frac{C_{od}}{C_{mig}} + \sqrt{\left(\frac{C_{od}}{C_{mig}}\right)^2 + \frac{C_{od}}{C_{oh}} + \frac{R_p}{C_{oh}}}. \qquad (28)$$

This reveals the dependence of optimal current density upon three trade-offs:

1. $\frac{C_{od}}{C_{mig}}$, the trade-off between osmosis and diffusion effects, and migration effects — with higher osmosis and diffusion driving higher current density to enhance productivity, ξ.
2. $\frac{C_{od}}{C_{oh}}$, the trade-off between osmosis and diffusion, and ohmic resistance — with higher ohmic resistance driving lower current density to enhance efficiency, η.
3. $\frac{R_p}{C_{oh}}$, the trade-off between the equipment-to-energy cost ratio and ohmic resistance — with higher specific equipment costs driving higher current density to reduce overall equipment costs

Fig. 7 provides a graphical illustration of Eq. (28) equations to further help understand the relationships between the three ratios above and the optimal current density. It is arrived at by considering the dependence of the four pre-factors C_{mig}, C_{od}, C_{mp} and C_{oh} in Fig. 6.

Considering Fig. 7 in combination with Eq. (28) we can see how, for fixed diluate salinity, high concentrate salinity leads to a higher optimal current density, as in Fig. 5d. Furthermore, we can see how, in particular at high concentrate salinity, the optimal current density increases with diluate salinity at low diluate salinity but decreases again at high diluate salinity.

5. Conclusions

Knowing the dependence of 'Local Cost*' upon salinity allows us to examine the cost of diverse ED systems. Figure 8 depicts four electrodialysis processes overlaid as pathlines on a (logarithmic) graph

[6]Note also that while osmosis, diffusion and electro-osmosis serve to reduce productivity (11), electro-osmosis acts in two opposing ways that mitigate its effect upon efficiency; as electro-osmosis increases C_{mig} in Eq. (23) decreases, decreasing efficiency, but C_{mp} in Eq. (26) also decreases, increasing efficiency. Thus the practical implications of electro-osmosis are to limit the maximum concentrate concentration and to reduce productivity but not to significantly affect efficiency.

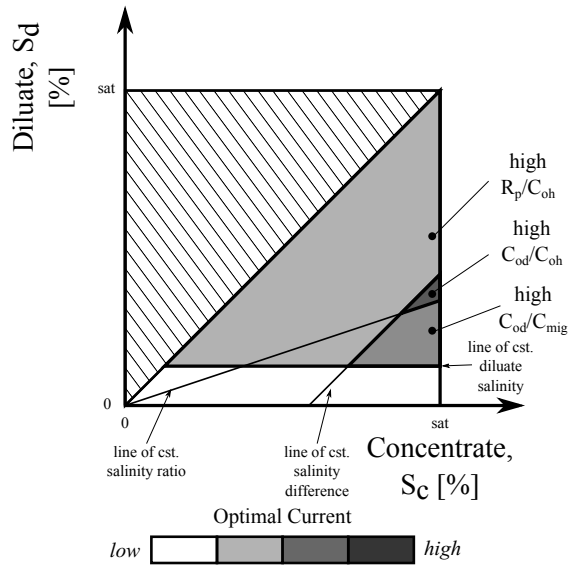

Figure 7: Optimal current density

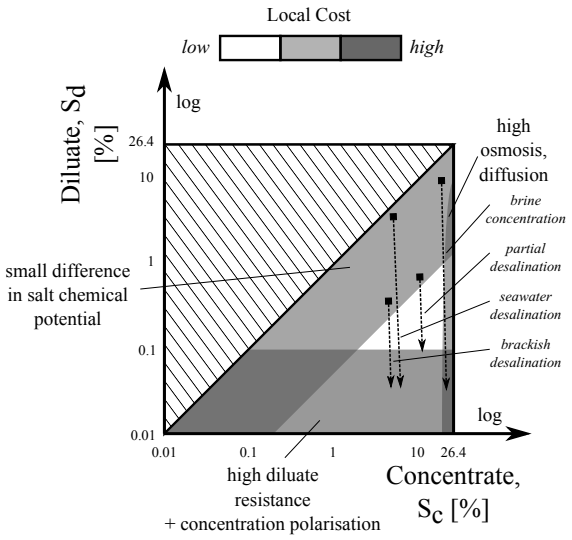

Figure 8: Graphical depiction of four electrodialysis processes

of 'Local Cost*'. From this figure we can draw the following conclusions:

- Brackish desalination is cost effective in its initial stage as the limiting current density remains reasonably high while the high salinity ratio lends itself to high productivity. By contrast, the final stages of salt removal are expensive as productivity is restricted by the limiting current density.

- The major difficultly faced in seawater desalination with electrodialysis is the low salinity ratio that persists during the majority of the process. This results in low productivity and efficiency.

- The ratio of concentrate-to-diluate salinity in brine concentration applications is low, resulting in low productivity and efficiency. Furthermore, depending on the concentrate concentration desired, osmosis and diffusion can further hamper performance particularly in the final stages of desalination (low diluate salinity).

- Of all processes, the most cost effective is partial brackish desalination, where a high-end brackish salinity stream is partially desalted. In such cases, both a high salinity ratio and a high diluate salinity can be maintained, allowing excellent productivity and efficiency. Such a process is of particular interest where a high purity product is not a requirement or where a polishing process such as reverse osmosis follows ED treatment. Examples of suitable applications might include the treatment of waters from coal-bed methane extraction [23], flue-gas desulphurisation or the treatment of low salinity produced waters in the oil and gas industry.

These results suggest there is promise in further developing electrodialysis for the treatment of waters from coal-bed methane, oil and gas extraction as well as flue-gas desulphurisation, where high-end brackish salinity streams are partially desalted.

6. Acknowledgement

The authors thank the King Fahd University of Petroleum and Minerals for funding the research reported in this paper through the Center for Clean Water and Clean Energy at MIT and KFUPM under project number R15-CW-11. Ronan K. McGovern is grateful for support via the Fulbright Science and Technology program sponsored by the U.S. Department of State, the International Desalination Associations Channabasappa Memorial Scholarship, the MIT Martin Fellowship for Sustainability and the Hugh Hampton Young Memorial Fellowship.

7. References

[1] J.-B. Lee, K.-K. Park, H.-M. Eum, C.-W. Lee, Desalination of a thermal power plant wastewater by membrane capacitive deionization, Desalination 196 (1) (2006) 125–134.

[2] S. J. Kim, S. H. Ko, K. H. Kang, J. Han, Direct seawater desalination by ion concentration polarization, Nature Nanotechnology 5 (4) (2010) 297–301.

[3] A. Mani, M. Z. Bazant, Deionization shocks in microstructures, Physical Review E 84 (6) (2011) 061504.

[4] M. Pasta, C. D. Wessells, Y. Cui, F. La Mantia, A desalination battery, Nano letters 12 (2) (2012) 839–843.

[5] S. Porada, B. Sales, H. Hamelers, P. Biesheuvel, Water desalination with wires, The Journal of Physical Chemistry Letters 3 (12) (2012) 1613–1618.

[6] K. N. Knust, D. Hlushkou, R. K. Anand, U. Tallarek, R. M. Crooks, Electrochemically mediated seawater desalination, Angewandte Chemie International Edition 52 (31) (2013) 8107–8110.
[7] H.-J. Lee, F. Sarfert, H. Strathmann, S.-H. Moon, Designing of an electrodialysis desalination plant, Desalination 142 (3) (2002) 267–286.
[8] P. Tsiakis, L. G. Papageorgiou, Optimal design of an electrodialysis brackish water desalination plant, Desalination 173 (2) (2005) 173–186.
[9] R. Yamane, M. Ichikawa, Y. Mizutani, Y. Onoue, Concentrated brine production from sea water by electrodialysis using exchange membranes, Industrial & Engineering Chemistry Process Design and Development 8 (2) (1969) 159–165.
[10] T. Seto, L. Ehara, R. Komori, A. Yamaguchi, T. Miwa, Seawater desalination by electrodialysis, Desalination 25 (1) (1978) 1–7.
[11] T. Sirivedhin, J. McCue, L. Dallbauman, Reclaiming produced water for beneficial use: salt removal by electrodialysis, Journal of membrane science 243 (1) (2004) 335–343.
[12] V. Nikonenko, A. Istoshin, M. K. Urtenov, V. Zabolotsky, C. Larchet, J. Benzaria, Analysis of electrodialysis water desalination costs by convective-diffusion model, Desalination 126 (1) (1999) 207–211.
[13] J. Wood, J. Gifford, J. Arba, M. Shaw, Production of ultrapure water by continuous electrodeionization, Desalination 250 (3) (2010) 973–976.
[14] G. Ganzi, Electrodeionization for high purity water production, in: AIChE Symposium series, Vol. 84, 1988.
[15] E. R. Reahl, Reclaiming reverse osmosis blowdown with electrodialysis reversal, Desalination 78 (1) (1990) 77–89.
[16] Y. Oren, E. Korngold, N. Daltrophe, R. Messalem, Y. Volkman, L. Aronov, M. Weismann, N. Bouriakov, P. Glueckstern, J. Gilron, Pilot studies on high recovery BWRO-EDR for near zero liquid discharge approach, Desalination 261 (3) (2010) 321–330.
[17] S. Thampy, G. R. Desale, V. K. Shahi, B. S. Makwana, P. K. Ghosh, Development of hybrid electrodialysis-reverse osmosis domestic desalination unit for high recovery of product water, Desalination 282 (SI) (2011) 104–108.
[18] M. Urtenov, A. Uzdenova, A. Kovalenko, V. Nikonenko, N. Pismenskaya, V. Vasil'eva, P. Sistat, G. Pourcelly, Basic mathematical model of overlimiting transfer enhanced by electroconvection in flow-through electrodialysis membrane cells, Journal of Membrane Science 447 (2013) 190 – 202.
[19] M. Turek, Dual-purpose desalination-salt production electrodialysis, Desalination 153 (1) (2003) 377–381.
[20] M. Fidaleo, M. Moresi, Optimal strategy to model the electrodialytic recovery of a strong electrolyte, Journal of Membrane Science 260 (1) (2005) 90–111.
[21] V. Zabolotskii, K. Protasov, M. Sharafan, Sodium chloride concentration by electrodialysis with hybrid organic-inorganic ion-exchange membranes: An investigation of the process, Russian Journal of Electrochemistry 46 (9) (Sept. 2010) 979 – 986.
[22] S. Koter, A. Cuciureanu, M. Kultys, J. Michałek, Concentration of sodium hydroxide solutions by electrodialysis, Separation Science and Technology 47 (9) (2012) 1405–1412.
[23] E. T. Sajtar, D. M. Bagley, Electrodialysis reversal: Process and cost approximations for treating coal-bed methane waters, Desalination and Water Treatment 2 (1-3) (2009) 284–294.
[24] R. K. McGovern, S. M. Zubair, J. H. Lienhard V, The benefits of hybridising electrodialysis with reverse osmosis.
[25] R. Robinson, R. Stokes, Electrolyte Solutions, Courier Dover Publications, 2002.
[26] K. Kontturi, L. Murtomaki, J. A. Manzanares, Ionic Transport Processes In Electrochemistry and Membrane Science, Oxford Press, 2008.
[27] T. Shedlovsky, The electrolytic conductivity of some uni-univalent electrolytes in water at 25 C, Journal of the American Chemical Society 54 (4) (1932) 1411–1428.
[28] J. Chambers, J. M. Stokes, R. Stokes, Conductances of concentrated aqueous sodium and potassium chloride solutions at 25 C, The Journal of Physical Chemistry 60 (7) (1956) 985–986.
[29] M. Fidaleo, M. Moresi, Electrodialytic desalting of model concentrated nacl brines as such or enriched with a non-electrolyte osmotic component, Journal of Membrane Science 367 (1) (2011) 220–232.
[30] A. Sonin, R. Probstein, A hydrodynamic theory of desalination by electrodialysis, Desalination 5 (3) (1968) 293–329.
[31] San Diego County Water Authority, Carlsbad desalination project (2012).
[32] U.S. Energy Information Administration, Annual energy outlook 2013, Tech. rep. (2013).
[33] A. Narebska, S. Koter, W. Kujawski, Ions and water transport across charged nafion membranes. irreversible thermodynamics approach, Desalination 51 (1) (1984) 3–17.
[34] A. Narebska, S. Koter, W. Kujawski, Irreversible thermodynamics of transport across charged membranes. Part I. macroscopic resistance coefficients for a system with nafion 120 membrane., Journal of membrane Science 25 (2) (1985) 153–170.
[35] S. Klein, F. Alvarado, Engineering equation solver, F-Chart Software (2013).
[36] B. Batchelder, W. W. Carson, L. Zhang, Electrodialysis system and process, uS Patent 8,142,633 (March 2012).

Nomenclature

Roman Symbols

a	activity, -
A_m	membrane permeability, l/m^2-h-bar
c	molar concentration, mol/l
C	concentration, mol/m^3
C_{cap}	production normalised equipment cost,\$/(m^3/day)
D	diffusion coefficient, m^2/s
E	potential, V
F	Faraday's constant, C/mol
G	Gibb's free energy, J
h	channel height, m
h_{fg}	latent heat of vaporisation, J/kg
i	current density, A/m^2
J	transmembrane molar flux, mol/m^2·s
K_Q	specific cost of equipment, \$/m^2
L_w	permeability to water, mol/m^2·s·bar
m	molal concentration, mol/kg solvent
MW	molecular weight, kg/mol
p	power density, W/m^2
P	pressure, bar
r	rate of return on capital, -
$\bar{r}$	area resistance, Ωm^2
R	universal gas constant, J/mol·K
R_p	price ratio, -
S	salinity, kg salt/kg solution
Sh	Sherwood number, -
T	temperature, K
t	solution transport number, -
T_s	membrane salt transport number, -
T_w	membrane water transport number, -
$\bar{T}$	integral ion transport number, -
V	voltage, V

$\bar{v}$	molar volume, m^3/mol

Greek Symbols

γ	molal activity coefficient, -
Δ	difference
η	efficiency, -
Λ	molar conductivity, Sm^2/mol
μ	chemical potential, J/mol
ν_s	number of moles of dissociated ions per mole of salt, -
ξ	productivity, W/m^2
Ξ	dimensionless cost, -
π	osmotic pressure, bar
ρ	density, kg/m^3
τ	time, years
ϕ	osmotic coefficient, -

Subscripts

am	anion exchange membrane
app	apparent
b	bulk
c	concentrate
cm	cation exchange membrane
cond	condensation
cp	cell pair
cu	counter ion
d	diluate
ev	evaporation
F	feed
lim	limiting
m	at membrane surface
mig	migration
i	counting index
j	junction
mp	membrane potential
oh	ohmic
os	osmotic
p	pump
pure	pure
s	salt
v	volumetric
w	water
0	reference value

Superscripts

am	anion exchange membrane
cm	cation exchange membrane
eo	electro-osmosis
o	osmosis
sw	seawater
1, 2	thermodynamic states
$\dot{}$	rate

Acronyms

CAF	capital amortisation factor
LCE	levelised cost of energy
MCS	marginal cost of separation